International Journal of Multiphase Flow 35 (2009) 261–269

Contents lists available at ScienceDirect

International Journal of Multiphase Flow

journal homepage: www.elsevier.com/locate/ijmulflow

Dynamics of short fiber suspensions in bounded shear flow

C. Jayageeth, Vivek Inder Sharma [1], Anugrah Singh *

Department of Chemical Engineering, Indian Institute of Technology Guwahati, Guwahati, Assam 781 039, India

ARTICLE INFO

Article history:
Received 2 September 2008
Received in revised form 23 October 2008
Accepted 10 November 2008
Available online 21 November 2008

Keywords:
Fiber suspension
Stokesian dynamics simulation
Bounded flow
Fiber orientation

ABSTRACT

We have studied the dynamics of non-colloidal short fiber suspensions in bounded shear flow using the Stokesian dynamics simulation. Such particles make up the microstructure of many suspensions for which the macroscopic dynamics are not well understood. The effect of wall on the fiber dynamics is the main focus of this work. For a single fiber undergoing simple shear flow between plane parallel walls the period of rotation was compared with the Jeffrey's orbit. A fiber placed close to the wall shows significant deviation from Jeffrey's orbit. The fiber moving near a solid wall in bounded shear flow follows a pole-vaulting motion, and its centroid location from the wall is also periodic. Simulations were also carried out to study the effect of fiber–fiber interactions on the viscosity of concentrated suspensions.

1. Introduction

Many industrial processes involve flow of suspensions of various sizes and shapes of particles. It is well understood that the properties of final product depends on the flow characteristics and rheology of suspensions. The particles used in these suspensions can be spherical, elongated or any arbitrary size. For elongated particles the mechanical properties of the final product depends on orientation and concentration distribution of the particles. Jeffery (1922) theoretically solved the motion of a single ellipsoidal particle undergoing simple shear flow in a Newtonian fluid. Subsequently, there have been several studies to determine the rheology of fiber suspensions (Mackaplow and Shaqfeh, 1996; Yamamoto and Matsuoka, 1994; Powell, 1991). However, most of zthese studies are limited to infinitely dilute or semi-dilute concentrations.

The study of the rheology of concentrated suspensions, in particular, their effective viscosity and its concentration dependence, is of general interest in material processing technology. In this study, we are concerned with numerical simulations of the suspension of non-spherical particles comprising of rigid spheres joined together. The dynamics of these particles which form anisometric particles are very different from the spherical particles. Anisometric particles have at least one distinguished direction along which their size is larger or smaller than perpendicular to it and the shape of the geometry is quantified by the aspect ratio. The shape of the particles has a large influence on the macroscopic properties of the suspensions and when the suspended particles are slender their orientations strongly affect the rheological properties of the flow. It is well known that the disturbance caused by the immersed particle decays as the distance from it increases, but the particle's motion is affected by other particles or walls in close proximity. Jeffery (1922) first developed the theory to describe the viscosity of dilute suspension of rigid ellipsoidal particles. Jeffery's equation for angular velocity of an ellipsoid in simple shear flow is

$$\dot{\theta} = -\frac{\dot{\gamma}}{r_e^2+1}(r_e^2\sin^2\theta + \cos^2\theta) \tag{1}$$

Here, r_e is the aspect ratio and θ is the angle of the ellipsoidal particle with respect to the flow direction. The dot represents the derivative with respect to time. It is quite clear from this expression that the angular velocity is maximum when $\theta = \pi/2$, that is the particle is oriented perpendicular to the flow, and it is minimum when $\theta = 0$, that is the particle has aligned itself parallel to the flow. This equation when integrated, gives the dependence of θ on time as

$$\tan\theta = \frac{1}{r_e}\tan\left[-\dot{\gamma}t\frac{r_e}{r_e^2+1} + \tan^{-1}(r_e\tan\theta_0)\right] \tag{2}$$

where θ_0 is the initial value of θ. The period of rotation for applied shear rate γ is given by

$$T = \frac{2\pi}{\dot{\gamma}}\left(\frac{r_e^2+1}{r_e}\right) \tag{3}$$

Arp and Mason (1977) have shown that Jeffrey's result will not hold due to particle–particle interactions if the dilute limit is exceeded. As the concentration of particles in the suspension increases, the interaction of the particles with other particles and with the walls of the container leads to other induced orientations.

* Corresponding author. Tel.: +91 361 2582259; fax: +91 361 2582291.
E-mail address: anugrah@iitg.ernet.in (A. Singh).
[1] Present address: Department of Nuclear Science and Engineering, MIT, 77 Massachusetts Avenue, Cambridge, MA 02139, USA.

0301-9322/$ - see front matter
doi:10.1016/j.ijmultiphaseflow.2008.11.002

Moreover, for a concentrated suspension, the instantaneous orientation of each particle is often unknown. Hence it is important to understand the dynamics of such particles in bounded flows and where particle–particle and particle–wall hydrodynamic interactions could be correctly accounted.

The numerical simulations to study the dynamics of anisometric particles employ regular particle shapes such as ellipsoids or spheroids. For elongated particles slender-body theory has been used in many studies. Another approach followed for the elongated particles is to treat it as spheres of equal size connected together in a chain like fashion. Yamamoto and Matsuoka (1995) presented a new method known as particle simulation method (PSM) to simulate the motion of fiber suspensions in shear flow at low Reynolds numbers without Brownian motion. They considered hydrodynamic interaction among fibers which are modeled by arrays of spheres present in a particle simulation cell wherein the motion of each constituent sphere of a fiber, which is dispersed into a unit cell with periodic boundaries, is followed to predict the microstructure and the rheological properties. They decomposed the hydrodynamic interaction into two parts, viz. intra- and inter-fiber ones. For Intra-fibers, they solved the many-body problem by calculating the mobility matrix for each fiber and this information was used to calculate the hydrodynamic force and torque exerted on each sphere. In the case of inter-fibers, they considered only the near-field lubrication force between spheres of one fiber and another. They observed an overshoot of suspension viscosity at the early stage for rigid fiber suspensions, but not for flexible ones. This was attributed to the transient change of the microstructure from the flow-directional orientation to the planar orientation of rigid fibers. Switzer and Klingenberg (2003) employed a particle-level simulation technique to investigate the rheology of non-Brownian, flexible fiber suspensions in simple shear flow. There model incorporates a variety of realistic features including fiber flexibility, fiber deformation, and frictional contacts. They found that the viscosity of fiber suspensions is strongly influenced by the fiber equilibrium shape, inter-fiber friction, and fiber stiffness. It was also found that the viscosity of the suspension increases as the fiber curvature, the coefficient of friction, or the fiber stiffness is increased. Pozrikidis (2005) investigated the significance of the particle aspect ratio on the statistics of the particle orientation and effective viscosity of a non-dilute suspension in simple shear flow using dynamic simulation. Numerical simulation based on an improved boundary-element method for particulate Stokes flow was used and an iterative procedure was adopted for particle contour traction and particle linear and angular velocities, based on particle-cloud clustering. Their results show the transition from a nearly-ordered state to a random configuration because of particle interactions and the particle eccentricity reduces the effective viscosity of suspension. Fan et al. (1998) used a numerical method to simulate fiber suspension in shear flow which takes into account short range interaction via lubrication forces and long range interaction via slender-body approximation, together with an appropriate Ewald summation technique. The macroscopic properties of suspension like Folgar–Tucker diffusion constant, the structure functions, and the reduced viscosity were analyzed. It is found that in the semi-concentrated to concentrated regime, the fibers no longer follow Jeffery's orbit and align mostly in shear direction. Claeys and Brady (1993) studied the hydrodynamic transport properties for the dispersions of prolate spheroids using the Stokesian dynamics numerical simulations. They examined the effect of concentration on hydrodynamic transport properties like sedimentation rate, hindered diffusivity and the rheological behavior of face-centered lattices. They also investigated the effect on microstructure of the dispersion by considering different arrangements of parallel ellipsoids. They found that the concentration dependence of the sedimentation rate reveals cooperative viscous interactions enhancing the collective rotational diffusion coefficient. While in the case of fibrous media the hindered diffusivities was found to decrease monotonically with density. Mackaplow and Shaqfeh (1996) employed a numerical technique to study the rheological properties of suspensions of rigid, non-Brownian slender fibers at zero Reynolds number based on the slender-body theory taking into account the inter-fiber hydrodynamic interactions. They studied suspension properties like extensional and shear viscosity for a variety of fiber aspect ratios and orientation distributions in the dilute and semi-dilute concentration regime. They found that the fiber–fiber interactions begin to enhance the stress in the suspension and it undergoes a transition to the semi-dilute regime well predicted by dilute theories. They also observed that in the semi-dilute regime, the dimensionless fiber disturbance screening length is only a function of suspension volume fraction and it was approximately the same for both aligned and isotropic suspensions, even though the latter contain many closer fiber–fiber interactions than the former. They found that the semi-dilute suspension screening length is independent of the fiber orientation distribution in the suspension.

There are few studies on wall bounded flows which focus on cross-streamline migration of fibers. Schiek and Shaqfeh (1997) have numerically investigated flow between two infinite, parallel plates separated by a distance comparable to the length of a suspended fibers and predicted the migration of fibers from region of low shear rate to high shear rate. Nitsche and Hinch (1997) predicted cross-stream migration of rigid rods undergoing diffusion and advection in parabolic flow between flat plates and observed that the fibers should migrate towards the wall. Gavze and Shapiro (1997) solved the boundary integral equation of Stokes flow to compute the hydrodynamic forces and velocities of spheroidal particles in a simple shear flow near a solid wall. The effect of wall is to create a non-zero velocity component in the normal direction to the wall and hence a spheroid moving in a shear flow near the wall will perform an oscillatory motion towards and away from the wall. They observed that the effect of wall decreases with increasing particle non-sphericity. Moses et al. (2001) conducted planar shear flow experiment to study the effect of boundaries on the fiber motion. They verified the motion of the fibers with the Jeffery's orbit for ellipsoidal particle. They observed that for distances less than a fiber length and greater than a fiber diameter from the wall, the fiber experiences an increased rate of rotation. They found that an increased effective shear rate can be used to match the fiber's orbit with the Jeffery's orbit. It was also found that the effective shear rate increased logarithmically with decrease in separation distance. The wall effect was found to be greater for longer aspect ratio fibers and fibers oriented perpendicular to the wall rotated faster than the one parallel to the wall at the same distance. Fibers which aligned with flow direction ceased to rotate. Holm and Soderberg (2007) conducted experiments to study the influence of shear close to a solid boundary on the fiber orientation in suspensions with different aspect ratios and concentrations.

Our aim in this work is to study the effect of wall on the dynamics of short fiber particles sheared between plane parallel walls using the Stokesian dynamics simulation (Brady and Bossis, 1988). The extension of Stokesian dynamics by Claeys and Brady (1993) for spheroidal particles incorporates increased mathematical complexities. Moreover, Mackaplow and Shaqfeh (1996) have argued that with increasing aspect ratio, higher order terms in multipole expansion becomes increasingly important but they are not included in the Stokesian dynamics. The method we have adopted uses spherical particles and hence present level of accuracy which includes two term expansion is accurate enough to capture near-field and far-field hydrodynamic interactions. In our simulations a rigid fiber particle consists of spherical particles held together by inter-particle forces. This enabled us to use the regular

Stokesian dynamics simulation for bounded shear flows which account for accurate particle–particle and particle–wall hydrodynamic interactions. In Section 2 we present our simulation method. The results in Section 3 provide detailed analysis of the trajectory of a single fiber moving near a plane wall in simple shear flow, the forces and torque the wall experiences due to fiber motion and the viscosity of suspension determined from the shear force on the wall.

2. Stokesian dynamics simulation method

In our earlier work (Singh and Nott, 2000) we have developed simulation method for wall bounded flows where the detailed methodology for bounded simulation can be found. The simulation method essentially uses the method of Nott and Brady (1994) to compute the far-field mobility interaction of particle–wall by considering the wall to be chain of particles. Exact sphere–wall interaction is used for lubrication interaction between sphere and wall in the resistance matrix (Durlofsky and Brady, 1989). Fig. 1 shows the simulation cell used in the present study to carry out dynamic simulation for bounded flow of chain of rigid particles. In order to simulate bounded plane shear, the suspension is restrained between two plane parallel walls translating relative to each other at a constant speed. This cell cannot, however, be replicated periodically in the *y*-direction, a constraint required for the Ewald summation in the far-field mobility interactions. Therefore, we have introduced a layer of fluid below the lower wall. When this cell comprising the layer of suspension restrained between the two walls and the layer of pure fluid, is replicated periodically in all directions, a negative shear rate is imposed on the suspension and a positive shear rate on the layer of fluid.

The velocities of the walls are fixed and the forces on them are determined while the forces on the particles are fixed and their velocities are to be determined from

$$R_{FU}^{SS}\cdot(U^S-\langle u\rangle)+R_{FU}^{SS}\cdot(U^S-\langle u\rangle)=F^S \tag{4}$$

where the superscripts *s* and *w* on the velocities and forces indicate sphere and wall quantities, and the superscripts *ss* and *sw* on the resistances (R_{FU}) indicate sphere–sphere and sphere–wall interactions, respectively. Similarly the forces on the walls are given by

$$R_{FU}^{WS}\cdot(U^S-\langle u\rangle)+R_{FU}^{WW}\cdot(U^W-\langle u\rangle)=F^W \tag{5}$$

The dynamics of the spheres and walls is determined, once the external force is specified by

$$F_{\text{hyd}}+F_{\text{ext}}=0 \tag{6}$$

In our simulations we impose inter-particle repulsive interaction between the particles, whose form is same as in the previous Stokesian dynamics simulations (Dratler and Schowalter, 1996; Nott and Brady, 1994)

$$F_{\alpha\beta}=F_0\frac{\tau e^{-\tau\epsilon}}{1-e^{-\tau\epsilon}}e_{\alpha\beta} \tag{7}$$

where $F_{\alpha\beta}$ is the force exerted by sphere β on sphere α. The parameters τ and F_0 specify the range of the force and its magnitude, respectively and ε is the separation between the surfaces. In order to simulate the rigid fibers which are made of spherical particles joined together, we have implemented the inter-particle forces in such a way that the spheres of a particle are always attached, though the whole fiber is free to translate and rotate. To do this we have considered attractive force between two spheres of a fiber particle if their velocities are in opposite directions but repulsive when their velocities are such that they would cause to move towards each other. For spheres of different fiber particle the form of inter-particle forces remain always repulsive as in the above equation. To restrict the rotation of individual particles of a fiber we also added restoring torque in the next time step if the angular velocity of the sphere deviated from zero. The value of the restoring torque was equal to the torque experienced by the individual sphere of a fiber in the previous time step. However, due to finite time step taken in the simulations there was small deviations and misalignment of particles. In order to avoid this we used correction scheme at the end of each time step. As per the scheme the correction is made only when the constituent spheres of the fibers deviate from straight line joining their centre. Based on the initial position of each constituent sphere the slope for each adjoining pair of spheres is calculated and compared for any deviation. If the slopes for all the adjoining spheres are not equal then based on the first and last sphere we calculate the required slope for positioning the rest of the spheres. Once the slope is known we position each sphere based on the position of the first sphere so that the centre-to-centre separation between two adjacent spheres is always $2a$.

Once U is known by solving Eq. (4), the positions (X^S) of the particles are determined by time integration of

$$\frac{dX_i^S}{dt}=U_i \tag{8}$$

Since the initial configuration X^S of the particles is known, the above equation upon integration determines the particle positions at the next time step. From the forces on the walls, the shear stress and hence the viscosity of suspension is easily determined

$$\sigma_{xy}=\frac{F_x^W}{A_W} \tag{9}$$

where F_x^w is the average x-component of the force on the wall and A_W is the total wall area for either wall. All the stresses are scaled by the shear stress $\eta\gamma$, where η is fluid viscosity and γ is the shear rate

$$\gamma=\frac{2U}{H} \tag{10}$$

Here, U is the speed of the wall and H is the channel width. In the mobility and resistance matrices, the components relating

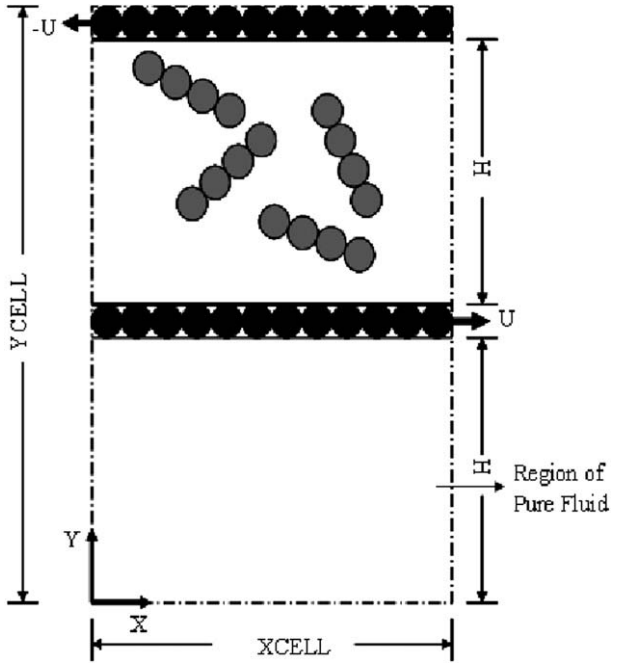

Fig. 1. A simulation cell showing the bounded shear flow of short fiber particles.

translational velocities to forces are scaled by $6\pi\eta a$ and those relating angular velocities to torque or stresslets by $6\pi\eta a^3$. In the simulations all distances are scaled by the particle radius a, the velocity by wall velocity U and time is scaled by a/U. The results presented in the following sections are in dimensionless units. The simulations carried out are for monolayer system, i.e. a fiber particle is only allowed to translate in x–y plane and rotate about z-axis. Hence we have studied the orientation of the fiber only about z-axis. This restriction of orientation in a single plane in monolayer simulations simplifies the problem and reduces the computational complexities without compromising on our objective of studying the wall effect on fiber dynamics.

3. Results

To validate the simulation method, we first studied the dynamics of a single rigid fiber of different aspect ratios in bounded shear flow. The motion of a single fiber was analyzed and its orbit was compared with the Jeffery's orbit for an ellipsoidal particle of equivalent aspect ratio. Simulations were carried out by placing the fiber at different initial locations from the wall. We analyzed the trace of fiber centroid for different aspect ratio fibers to verify the pole-vaulting behavior of the fiber close to the wall. Finally the relative viscosity was compared for fiber and spherical suspensions.

3.1. Trajectory of a single particle

Fig. 2 shows the schematic of a fiber placed between two plane parallel walls moving with equal and opposite velocities to produce a simple shear flow. Chain of spheres connected together were placed perpendicular to the flow direction and positioned between the two walls. The location and orientation of each fiber with time was computed.

Ideally, for unbounded shear flow of fiber the time-period of rotation should match well with the Jeffery's orbit. This was verified by keeping the distance of separation between the walls very large. When the fiber is located close to the wall there is significant deviations in the time-period from the Jeffrey's orbit (Fig. 3). It is to be noted that the Jeffrey's result is valid for ellipsoidal particle in unbounded shear flow. Bretherton (1962) has shown that the motion of a cylindrical rod was equivalent to that of an ellipsoidal particle of an equivalent aspect ratio instead of the aspect ratio of the cylinder. We have used the semi-empirical relation for the equivalent ratio given by Harris and Pitman (1975) to make comparison with the Jeffrey's orbit

$$r_e = 1.14 a_r^{0.844} \tag{11}$$

In the above expression, a_r is the true aspect ratio of any particle with fore-aft symmetry and for our case, $a_r = N_{\text{fib}}$, where N_{fib} is the total number of spherical particles in a single fiber.

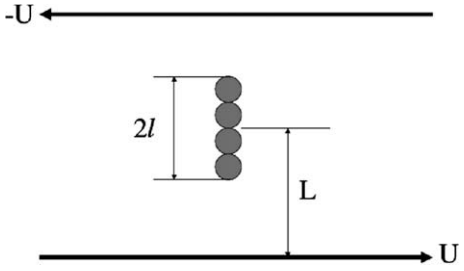

Fig. 2. A single fiber of length $2l$ sheared between two plane parallel walls whose centroid is located at a distance of L from the wall.

The simulation results show that the deviation in the orbit of rotation of a fiber close to wall increases as its distance from wall decreases. This departure from the Jeffery's orbit can be attributed to the effect of wall on fiber motion. When the fiber is close to the wall it tends to orient in the flow direction parallel to the wall. Far away from the wall the fiber experiences less wall effect. Consequently, it takes less time to complete one orbit rotation. The time-period is found to increase with aspect ratio. Also we observe that for a given separation distance relative to the wall, the fiber orbit moves further away from Jeffery's orbit as the aspect ratio is increased. This is because; the higher aspect ratio fiber spends longer time aligning parallel to the flow direction. Small discrepancies even at large distance could be due to the fact that the equivalent aspect ratio taken was for cylindrical fiber which had blunt end whereas the fibers in our simulation has rounded ends.

From the comparison of time-period for different aspect ratios (Fig. 4) it is clear that there is an apparent increase in the time-period when the fiber is close to the wall ($L/2l < 1$). As the relative distance from the wall i.e. $L/2l$ increases, the time-period is found to be very close to Jeffery's orbit. In all our simulations, we have considered the wall to be a plane one with proper lubrication force included when the particle is close to the wall. Also, we have kept the shear rate constant for all simulation runs. There are very few works related to the study of boundary effects on the orientation and rheological properties of fiber suspensions. Moses et al. (2001) have experimentally studied the effect of wall on the motion of single fiber of different aspect ratios and have found that the fiber experiences enhanced shear and increased rate of rotation close to the wall. Also they observed that higher aspect ratio fibers rotated faster near the wall than those with lower aspect ratio fibers. They used a translational model to justify that a fiber oriented perpendicular to the wall experiences a higher effective shear rate than a fiber oriented parallel to the wall at the same separation distance.

In Fig. 5, we have shown the variation of the location of the centroid of a fiber with time. Stover and Cohen (1990) experimentally studied the fiber motion in a plane Poiseuille flow and observed that the fibers aligned with the flow direction and within less than half a fiber's length from the wall, remained there indefinitely. They also reported that fibers in the near wall region performed a motion which could be described as pole-vaulting and centroid of the fiber moved away from the wall periodically. Our results for the bounded shear flow are in support with the findings of Stover & Cohen. The centroid of the fiber shows some periodic undulations when it is close to the wall. The undulations reduce far away from the wall. In the case of fiber of aspect ratio $a_r = 2$ (Fig. 5a) we see very little variation in the position of the centroid for separation from wall, $L/2l > 1$. When the fiber is close to the wall ($L/2l = 0.75$), then the centroid shows small undulations in its position. In the case of fiber of aspect ratio $a_r = 4$ (Fig. 5b), centroid remains at the same lateral position when it is far away from the wall ($L/2l = 2.5$), but shows periodic undulations as the separation from the wall is reduced ($L/2l = 0.625$). The undulation of fiber centroid is more apparent for higher aspect ratio fibers. For fiber of aspect ratio, $a_r = 6$ (Fig. 5c) we see that the centroid shows less movement from its initial position when $L/2l = 1.667$, but close to the wall ($L/2l = 0.667$) the motion of centroid shows clear offset from its mean position. For $a_r = 8$ (Fig. 5d) we see clear periodic motion of the fiber centroid for $L/2l = 0.625$ and $L/2l = 0.75$. Thus it can be concluded that as the relative separation distance from the wall is increased or when the fiber is more than a fiber length away from the wall then the effect of wall is less. For distances less than a fiber diameter the wall effect becomes more pronounced. Higher aspect ratio fiber takes longer time to complete one rotation than the lower aspect ratio fibers for the same relative separation distance from the

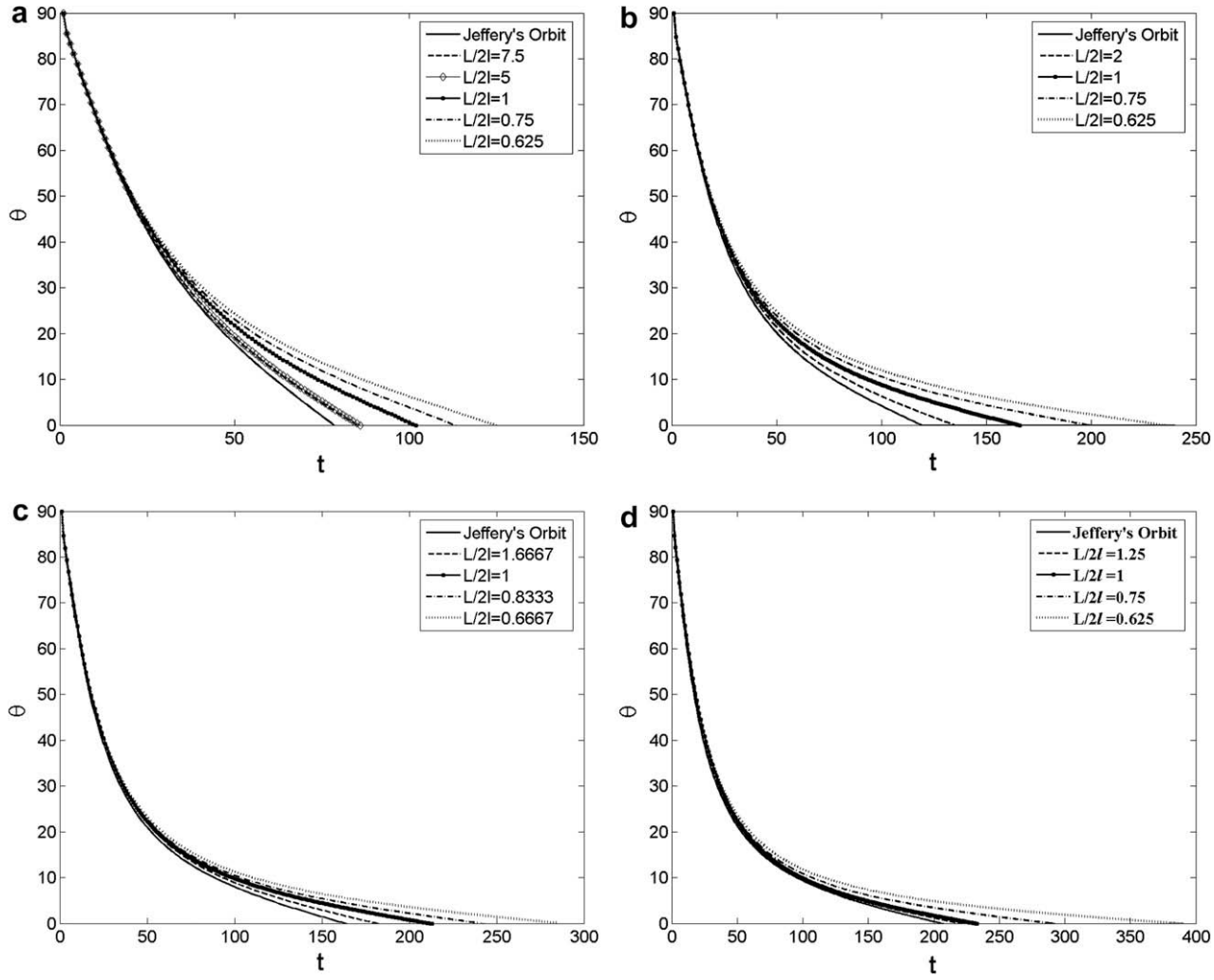

Fig. 3. Trajectory of a single fiber near a plane wall for different aspect ratios (a) $a_r = 2$, (b) $a_r = 4$, (c) $a_r = 6$ (d) and $a_r = 8$.

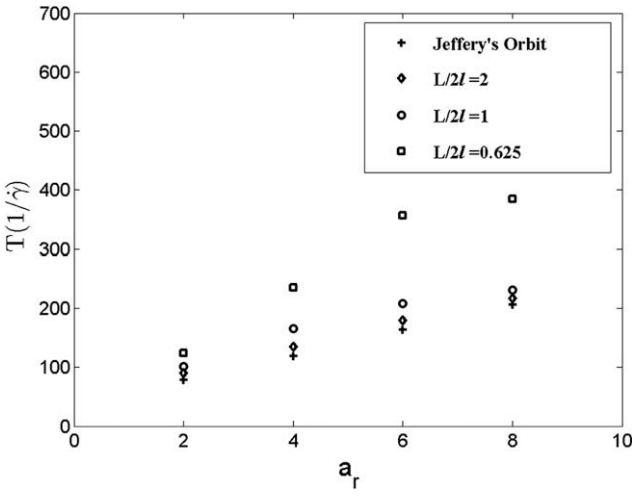

Fig. 4. Comparison between simulated and theoretical periods (Jeffrey's orbit) of rotation of a rigid fiber for different centroid location from the wall as a function of aspect ratio.

wall. Stover & Cohen have argued that the non-hydrodynamic interaction between the fiber and the wall causes the pole-vaulting motion. In our simulations there were no forces of the kind shown in Eq. (7) employed between the particle and wall but still we are able to capture the motion observed experimentally. It appears that the bumpy wall formulation in mobility matrix is not over simplification but represents the non-smooth nature of surfaces present in real situations. It is this rough wall which could be responsible of any non-hydrodynamic effects. Another important information which can be gathered from Fig. 5d is that observing the period of oscillation of the centroid position we can further confirm the observations in Fig. 3 that as the fiber moves away from the wall its time-period of rotation decreases. We would also like to point out that in Fig. 5b and 5d at some times the centroid position is slightly higher than the minima expected. This occurs at the time when the fiber starts crossing the periodic boundary in the flow direction. The periodic boundary is implemented such that if a particle of fiber crosses right boundary of the cell it enters from the left boundary but at the same y-location thus restricting y-positioning due to any lift forces. For such particle if the rotation was bringing the centroid downward the adjustment in the periodic position would cause it to move slightly upward due to correction scheme as explained in Section 2. This aberration can be removed when the cell length in the flow direction is taken very large so that several rotations are complete within one periodic cell length but this would invite more computational cost. The use of very small time step is

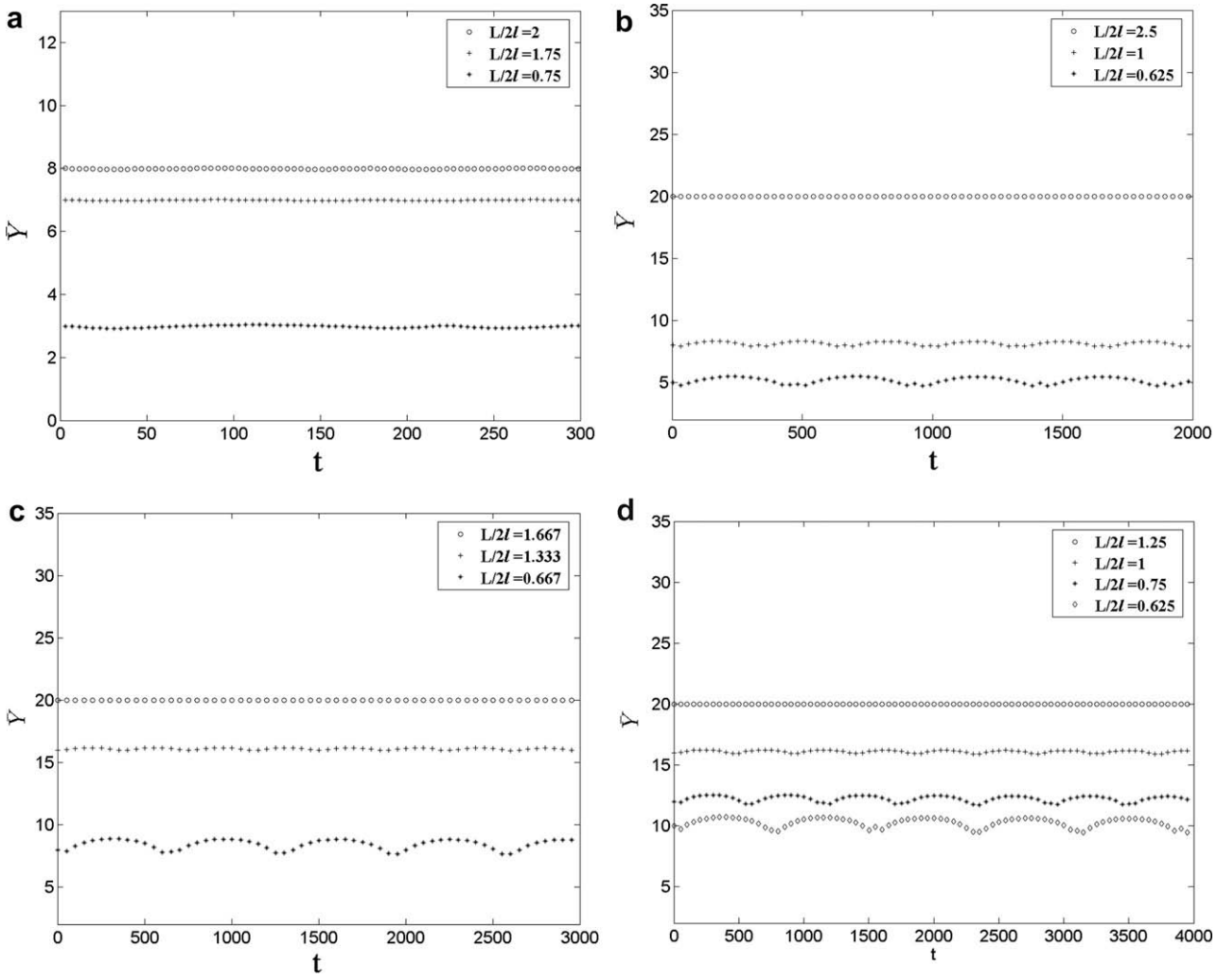

Fig. 5. Time trace of the centroid of a single rigid fiber near a plane wall for various location of its centroid from the wall. The aspect ratios of the fibers in the figures are (a) $a_r = 2$, (b) $a_r = 4$, (c) $a_r = 6$ and (d) $a_r = 8$.

another way to remove this noise but again at the increased computational cost.

3.2. Force and torque on the wall due to fiber motion

Periodic rotation of a fiber close to a plane wall gives rise to force and torque on the wall which also shows periodic variations. We observe from Fig. 6 that the normal force values though small, are more for high aspect ratio fibers as compared to low aspect ratio fibers for the same initial centroid location from the wall. The lift force (F_y) is the least when the fiber is aligned parallel or perpendicular to the wall. The maxima is observed at an orientation of $\theta = 60^\circ$ where the asymmetry of the flow field near the particle is the largest. In Fig. 6 the angle for the maximum value of F_y depends slightly on the aspect ratio but the difference is small. The maximum for higher aspect ratio fiber is observed to be at an angle slightly less than 60°. This could be due to the effect of other wall on the fiber rotation. The dimensionless gap width in all the simulations was taken as 40. For low aspect ratio fibers placed close to one wall, the effect of other wall would be small but for higher aspect ratio it may have slight influence on the fiber motion and this may be the cause of difference unless we keep the gap width much larger. The effect of aspect ratio and relative separation distance from the wall on torque as a function of fiber orientation angle is given in Fig. 7. The maxima and minima explained here are in context with the magnitude of the torque on the wall which is negative in this case for most part of the orientation angle. The torque

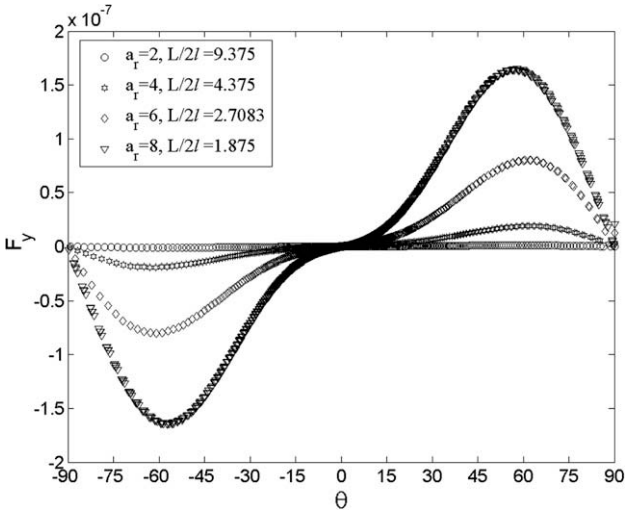

Fig. 6. Lift force on the wall (F_y) versus orientation angle (θ) for rigid fibers of various aspect ratios.

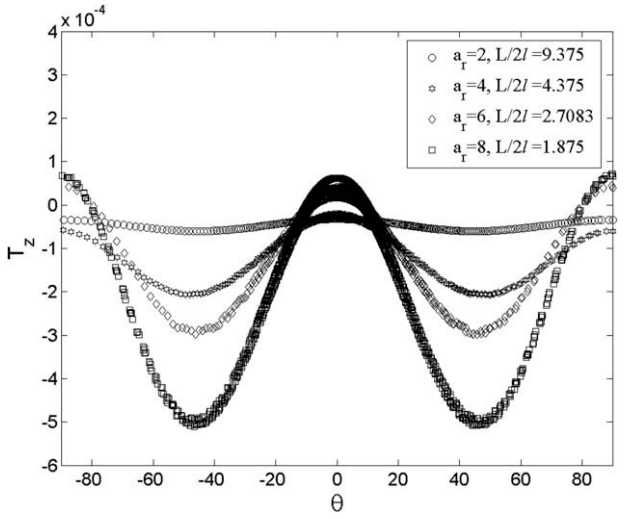

Fig. 7. Torque on the wall (T_z) versus orientation angle (θ) for rigid fibers of various aspect ratios.

on the particle will be equal and opposite of that on the wall. We observe that the maximum in the magnitude of the torque is observed at 45° whereas the minimum is expected at 0° and 90°. When the fiber is aligned parallel to the wall ($\theta = 0°$), it offers minimum resistance and hence the torque is also minimum. For the upright position of the fiber ($\theta = 90°$), the effect of wall on the flow near a fiber in such a position is to slow down the fluid motion over the particle edge facing the wall thus reduced viscous friction and torque on the wall. The maximum is expected at the intermediate position of $\theta = 45°$. For low aspect ratio fibers ($a_r = 2, 4$) the torque value is indeed close to zero at 0° and 90° but for aspect ratio 6 and 8 the torque value is small but slightly positive. This could be attributed to the presence of the other wall on the fiber motion as explained above. The shear force (F_x) gives the measure of viscosity of suspension and its dependence on orientation angle is discussed in the next section.

3.3. Viscosity of short fiber suspensions

Variation of relative viscosity as a function of time for different aspect ratio fibers was also analyzed. First we have analyzed the system of infinitely dilute suspension. For this case a single particle was sheared between plane parallel walls. Since the simulation employs periodic boundary condition, even a single fiber particle in the simulation cell is equivalent to a system of perfectly ordered but very dilute suspension. In such system each particle executes periodic rotation with varying angular velocity over the time-period. In Fig. 8a the viscosity value is plotted against the fiber orientation angle. It can be observed that the viscosity shows minima when the fiber is oriented either parallel or perpendicular to the wall. When the orientation is around 45° the viscosity value shows maxima. When the fiber is aligned parallel to the wall it offers minimum resistance. The effect of wall on fiber motion is such that when the fiber is parallel it slows down the flow in the gap between the particle and the wall and hence reduces the viscous friction. On the other hand when the particle is in an upright position (perpendicular to the flow and wall) it experiences a torque which stems from the flow speedup around its surface. The effect of wall on the flow near a fiber in such a position is to slow down the fluid motion over the particle edge facing the wall. This causes the reduction of viscous drag force on the wall and hence the reduced viscosity of suspension. The maximum value of viscosity is observed at the intermediate position of $\theta = 45°$. This tendency is also predicted by Jeffrey's equation for ellipsoidal particles. It can be noticed that the increase in viscosity is mainly caused by the translational friction force between particle and fluid, and the contribution of rotational frictional torque is minimum. Fig. 8b shows the time trace of viscosity value. From this we can infer that the effect of fiber–fiber interaction is less in infinitely dilute fiber suspension and fiber moves periodically about its relative position showing a dominant frequency and a corresponding time-period of rotation. The effect of fiber–fiber interaction becomes dominant only at moderately higher concentrations. It can be observed that a fiber has minimum angular velocity when it is aligned to the flow direction and hence it spends more time about the orientation angle 0°. As soon as the fiber reaches 45°, it quickly rotates to perpendicular position (90°) at which its angular velocity is maximum. We can also notice that the relative suspension viscosity is close to the pure Newtonian fluid value in accordance with the Einstein's formula for relative suspension viscosity for infinitely dilute suspension of spherical particles. We have also analyzed the power spectrum of the viscosity data for dilute and concentrated suspension (not shown here). For infinitely dilute system the peak value correspond to the time-period of rotation. When the particle fraction increases fiber–fiber interaction destroys the periodic orbits and the power spectrum shows peaks of various frequencies. On the other hand as particle interactions become much higher, the particles are more likely to be oriented in the direction of the shear flow rather than in the normal direction (Pozrikidis, 2005).

Fig. 9 shows the time trace of relative viscosity of concentrated suspensions at various areal fractions. The mean area fraction is defined as

$$\phi = \frac{N_I \pi a^2}{H L_x} \tag{12}$$

where N_I is the total number of interior spheres (excluding the wall particles) in the simulation cell and L_x is the cell length in x-direction. From the Fig. 9 we observe that for dilute concentrations the peaks in the viscosity values occur at regular intervals indicating that the periodicity is preserved. At higher concentration this periodicity is destroyed due to fiber–fiber interactions and we observe irregular peaks.

At higher concentrations the fiber viscosity is initially higher due to randomly dispersed fibers but decreases later as the particles align towards the shearing plane. It was found that the variance of relative viscosity increases with areal fraction. Also the variance of relative viscosity for fiber suspension of $a_r = 4$ is greater than that of fiber suspension of $a_r = 2$.

Fig. 10 presents a comparison of the relative viscosity of suspension of spherical particles and rigid fibers of aspect ratio 2 and 4. Since our simulations are for 2-D flow the suspension microstructure has only orientation in velocity–velocity gradient plane. Though this appears to be highly restrictive, such microstructures are realized in film flow and thin channel flow. We observe that at low and moderate concentrations the fiber suspension viscosity is relatively larger than the spherical particles. Given the particle areal fraction, the relative suspension viscosity increases as the particles become more elongated, over a broad range of areal fractions. It is apparent that for low aspect ratio fibers in the dilute to semi-concentrated regime, the volume fraction influences the relative viscosity primarily, and the effect of aspect ratio being secondary. We also observe that at higher fraction, the fibers are more aligned and hence the effect of aspect ratio on viscosity diminishes. Our results are in agreement with the observations of Claeys and Brady (1993) but in contrast with the numerical simulations of Pozrikidis (2005).

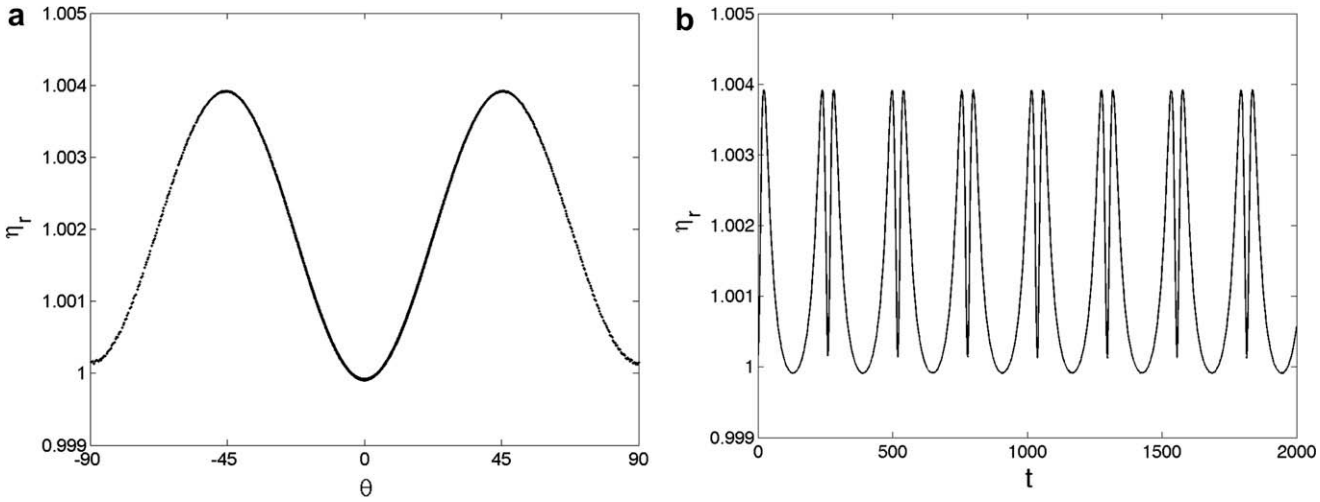

Fig. 8. (a) Variation of viscosity with orientation angle. (b) Time trace of relative viscosity of infinitely dilute suspension. The fiber aspect ratio a_r was 4 and the areal fraction was 0.002 in this simulation. The values of repulsive force parameters, F_0 and τ were taken as 0.01 and 100.

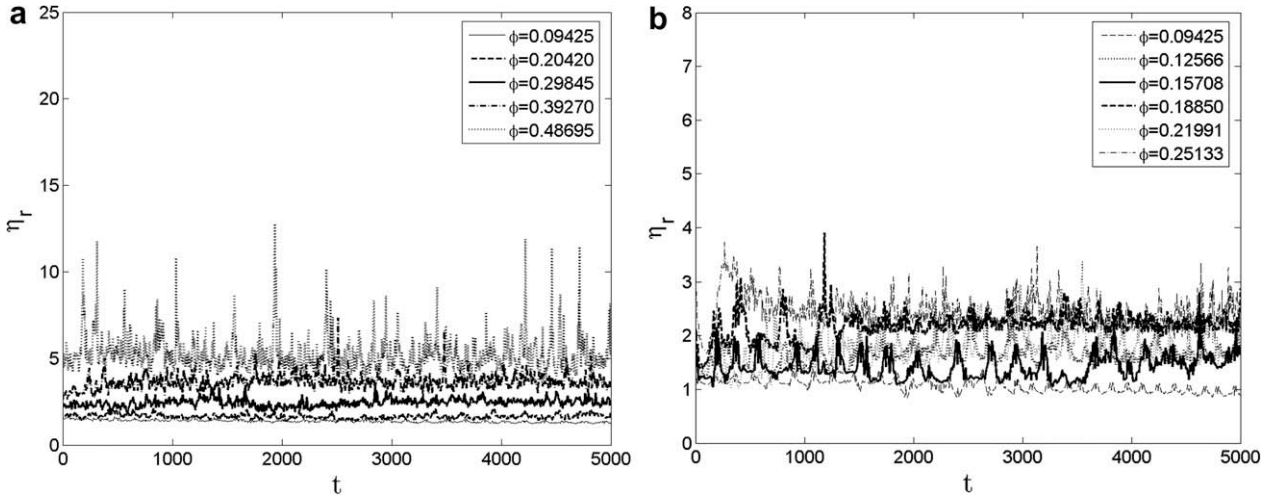

Fig. 9. Time trace of relative viscosity of concentrated suspensions at various areal fractions. The aspect ratio in the figures are (a) $a_r = 2$, (b) $a_r = 4$. The other parameters were same as in Fig. 8.

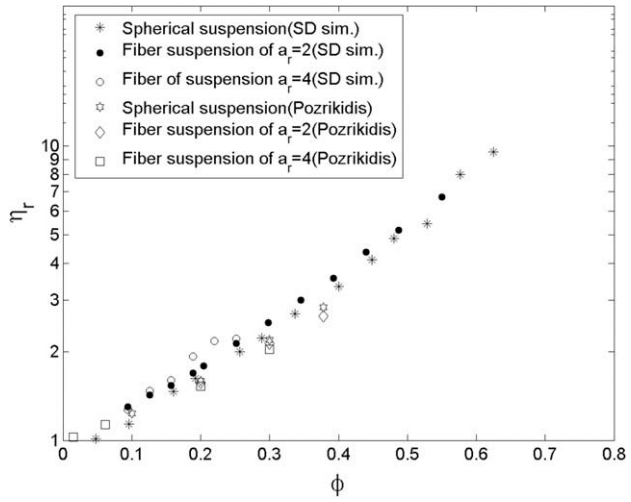

Fig. 10. Plot of relative suspension viscosity versus particle areal fractions for spherical and rigid fiber suspension of aspect ratio 2 and 4.

They observed that the viscosity of isotropic dispersion rapidly increases as the particle aspect ratio is increased. The disagreement could be due to the fact that their simulations take an initially ordered suspension which evolves to random orientations. In our simulations we have taken random initial configuration of the fibers. The increase in the viscosity with aspect ratio has been argued in many literatures. Arp and Mason (1977) have shown that the spin of a sphere close to a boundary is always greater than that of elongated particle. At low and moderate concentration the spherical suspension would offer less resistance to the boundary for this reason. On the other hand a fiber would be restrained to spin freely due to presence of other fiber in concentrated suspension and hence the higher viscosity. Gavze and Shapiro (1997) have numerically studied the motion of a fiber near a plane wall using boundary integral method and observed that the rotational-translational coupling is affected by the wall. They also found that the wall retards the fiber motion and fiber close to the wall had longer periods between rotations. These factors contribute to higher viscosity observed with suspension of elongated particles.

4. Conclusion

We have performed Stokesian dynamics simulations to study the dynamics of rigid non-Brownian fibers in bounded shear flow between plane parallel walls. The effect of relative separation from the wall on the motion of single fiber of equivalent aspect ratio was studied by comparing the fiber orbit with the Jeffery's orbit. When the relative separation distance from the wall is large, the fiber orbit is closer to the Jeffery's orbit, which indicates that the simulation method captures the dynamics of rodlike particles. We found that the time-period of rotation considerably increases as the fiber is close to the wall and the fiber spends longer time aligned parallel to the flow direction. The time-period for rotation is found to increase with aspect ratio. Presence of wall creates a velocity component normal to the wall and the fiber performs periodic motion towards and away from the wall. This pole-vaulting motion is more apparent for higher aspect ratio fibers placed close to the wall. The force and torque on the wall is strongly influenced by the fiber orientation. The wall effects are more pronounced for higher aspect ratio fibers. We have also computed the viscosity of short fiber suspensions from the knowledge of wall shear stresses. For infinitely dilute system the viscosity value shows periodic fluctuations which become irregular at higher concentrations due to fiber–fiber interactions. Viscosity values for suspension of elongated particles are higher compared to the spherical suspension which is in agreement with previous studies on such systems. The method presented in our work can be easily extended to flexible fibers.

References

Arp, P.A., Mason, S.G., 1977. The kinetics of flowing dispersions VIII Doublets of rigid spheres (theoretical). J. Colloid Interf. Sci. 61 (1), 21–43.

Brady, J.F., Bossis, G., 1988. Stokesian dynamics. Annu. Rev. Fluid Mech. 20, 111–157.

Bretherton, J.P., 1962. The motion of rigid particles in a shear flow at low Reynolds number. J. Fluid Mech. 14, 284–304.

Claeys, I.L., Brady, J.F., 1993. Suspensions of prolate spheroids in Stokes flow. Part 1 dynamics of finite number of particles in an unbounded fluid. J. Fluid Mech. 251, 411–442.

Dratler, D.I., Schowalter, W.R., 1996. Dynamic simulation of suspensions of non-Brownian hard spheres. J. Fluid Mech. 325, 53–77.

Durlofsky, L., Brady, J.F., 1989. Dynamic simulation of bounded suspensions of hydrodynamically interacting particles. J. Fluid Mech. 200, 39–67.

Fan, X., Phan-Thien, N., Zheng, R., 1998. A direct simulation of fibre suspensions. J. Non-Newton. Fluid Mech. 74, 113–135.

Gavze, E., Shapiro, M., 1997. Particles in a shear flow near a solid wall: Effect of nonsphericity on forces and velocities. Int. J. Multiphas. Flow 23 (1), 155–182.

Harris, J.B., Pitman, J.F.T., 1975. Equivalent ellipsoidal aspect ratios of slender rod-like particles. J. Colloid Interf. Sci. 50 (2), 280–282.

Holm, R., Soderberg, D., 2007. Shear influence on fiber orientation. Rheol. Acta 46, 721–729.

Jeffery, G.B., 1922. The motion of ellipsoidal particles immersed in a viscous fluid. Proc. Roy. Soc. Lond., Ser. A 102, 161–179.

Mackaplow, M.B., Shaqfeh, E.S.G., 1996. A numerical study of the rheological properties of suspensions of rigid, non-Brownian fibres. J. Fluid Mech. 329, 155–186.

Moses, K.B., Advani, S.G., Andreas, R., 2001. Investigation of fiber motion near solid boundaries in a simple shear flow. Rheol. Acta 40, 296–306.

Nott, P.R., Brady, J.F., 1994. Pressure driven flow of suspensions: simulation and theory. J. Fluid Mech. 275, 157–199.

Nitsche, L.C., Hinch, E.J., 1997. Shear-induced lateral migration of Brownian rigid rods in parabolic channel flow. J. Fluid Mech. 332, 1–21.

Pozrikidis, C., 2005. Orientation statistics and effective viscosity of suspensions of elongated particles in simple shear flow. Eur. J. Mech. B/Fluid. 24, 125–136.

Powell, R.L., 1991. Rheology of suspension of rodlike particles. J. Stat. Phys. 62, 1073–1094.

Schiek, R.L., Shaqfeh, E.S.G., 1997. Cross streamline migration of slender, Brownian fibers in plane poiseuille flow. J. Fluid Mech. 332, 23–39.

Singh, A., Nott, P.R., 2000. Normal stresses and microstructure in bounded sheared suspensions via Stokesian dynamics simulations. J. Fluid Mech. 412, 279–301.

Stover, C.A., Cohen, C., 1990. The motion of rodlike particles in the pressure-driven flow between two flat plates. Rheol. Acta 29, 192–203.

Switzer, L.H., Klingenberg, D.J., 2003. Rheology of sheared flexible fiber suspensions via fiber-level simulations. J. Rheol. 47 (3), 759–778.

Yamamoto, S., Matsuoka, T., 1994. Viscosity of dilute suspensions of rodlike particles: a numerical simulation method. J. Chem. Phys. 100 (4), 3317–3324.

Yamamoto, S., Matsuoka, T., 1995. Dynamic simulation of fiber suspensions in shear flow. J. Chem. Phys. 102 (5), 2254–2260.